SEA ICE MAPPING ALGORITHM FOR QUIKSCAT AND SEAWINDS

Quinn P. Remund and David G. Long
Brigham Young University, MERS Laboratory
459 CB, Provo, UT 84602
801-378-4884, FAX: 801-378-6586 remundq@ee.byu.edu

Abstract— Polar sea ice extent is an important input to global climate models and is considered to be a sensitive indicator of global climate change. Studies have shown that Ku-band scatterometer data are sensitive to the presence of sea ice. An algorithm has been developed for sea ice extent detection using data from the NASA scatterometer (NSCAT). This paper discusses the extension of that algorithm to data from future scatterometers, QuikSCAT and Seawinds. Simulated Seawinds data are generated from NSCAT data. Experiments are conducted using Seawinds data as inputs to the NSCAT algorithm. The results show that these data can be used to estimate the ice edge although with a lower degree of accuracy than when NSCAT σ^o data are used. While NSCAT requires 6 days of data to effectively implement the algorithm, Seawinds will only require 1-2 days of data due to the wider swath, lack of a nadir gap, and better single pass cell overlap.

INTRODUCTION

Mapping the extent of sea ice in the earth's polar regions is of great interest to the scientific community. Sea ice is considered to be a sensitive indicator of global climate change. It is also used as an input to global weather and climate models. In recent years, remote sensing using spaceborne instruments has proven invaluable in studying the polar regions [1]. In particular, Ku-Band scatterometer data have been used to detect polar sea ice [2]. Ku-band σ^o response over polar regions is a function surface roughness, water content, and ice type. These data may be used to determine surface properties of polar regions.

An algorithm has been developed to map the extent of sea ice using σ^o measurements from the NASA scatterometer (NSCAT) [3]. The resulting ice map closely matches the NSIDC SSM/I-derived 30% sea ice concentration extent. Unfortunately, the loss of NSCAT in June 1997 limits the use of this algorithm. However, the ice detection technique can be applied to σ^o data from future Ku-band scatterometers such as QuikSCAT and Seawinds. QuikSCAT is scheduled for launch in November 1998 and is virtually identical in design to Seawinds which will be deployed in early 2000. Although the QuikSCAT and Seawinds instruments differ from NSCAT, the ice mapping algorithm can be modified to operate for them as well.

This paper is organized as follows. In section two, the necessary background is discussed. Section three describes the application of the ice detection algorithm to simulated Seawinds data and compares the results to NSCAT ice detection. The conclusions are given in section four.

BACKGROUND

The NSCAT [4] and Seawinds [5] instruments differ in several ways. NSCAT is a dual polarization fan beam scatterometer. The fan beam footprint on the earth's surface is further resolved in range through Doppler filtering [4]. Hence, σ^o measurements are obtained at both polarizations from 10° to 60° incidence. On the other hand, Seawinds is a dual polarization scanning pencil beam scatterometer. The inner scan is at 47° incidence and is horizontally polarized while the outer scan operates at 55° and is vertically polarized. Like NSCAT, Doppler filtering is used to increase the spatial resolution of the σ^o measurements.

While the nominal resolution of these instruments is not conducive to some land and ice studies, a resolution enhancement technique, the scatterometer image reconstruction with filter (SIRF) algorithm, can be used to increase the resolution to 5-10 km [6]. This method uses the overlap of σ^o measurements from multiple beams and multiple passes of the satellite to reconstruct the data to higher resolution (5-10 km).

Over a limited incidence angle range of [20°, 55°], σ^o (in dB) is approximately a linear function of θ,

$$\sigma^o(\theta) = \mathcal{A} + \mathcal{B}(\theta - 40°) \tag{1}$$

where A and B are functions of surface characteristics, azimuth angle, and polarization. A is the σ^o value at 40° incidence and B describes the dependence of σ^o on θ. A and B provide valuable information about surface parameters. 40 degrees is chosen as a mid-swath value, but any interior swath angle can be used. The SIRF algorithm produces both A and B images from NSCAT or Seawinds σ^o measurements. Six days of NSCAT data are required to produce good A and B images for the polar regions due to the low number of horizontal polarization data. In contrast, Seawinds has no nadir gap and a wider swath increasing the overall coverage and decreasing the amount of time needed to produce SIRF reconstructed σ^o images. For Seawinds, only 1-2 days of data will be required to produce the polar images.

Three parameters are used in the NSCAT sea ice discrimination algorithm: the polarization ratio (γ), the vertical polarization incidence angle dependence (B_v), and

0-7803-4403-0/98/$10.00 © 1998 IEEE

the vertical polarization σ^o estimate error standard deviation (κ). The polarization ratio is defined by the equation

$$\gamma = A_v / A_h \tag{2}$$

and measures the polarization response of the surface [2]. Due to differences in scattering characteristics, γ is generally high for ocean and low for sea ice [2]. B_v is the incidence angle dependence of σ^o as described above. Ocean and ice have low and high B_v values, respectively. The final parameter, κ, is the standard deviation of the ensemble of differences of each σ^o measurement with its associated forward projection:

$$\kappa = \sqrt{\sum_l (\sigma_l^o - \hat{\sigma}_l^o)^2} \tag{3}$$

where the σ_l^o are the vertical polarization measurements touching the pixel of interest. The κ parameter is a measure of σ^o temporal dependence and azimuthal modulation: ocean has high κ values while ice κ is generally lower.

In the NSCAT algorithm, γ and B_v are used as the primary classification parameters. The distribution of γ vs. B_v is bimodal with the modes corresponding to ice and ocean pixels. The modes are separated using both linear and quadratic boundaries in the γ vs. B_v plane. Figure 1 shows an example γ vs. B_v distribution contour plot illustrating the decision boundaries for the two methods. Errors occur due to high wind events over the ocean and other physical mechanisms. The errors are corrected by using a threshold on κ for all pixels for which the linear and quadratic estimates disagree. For a more detailed description of the algorithm, see [3]. The ice extent estimate obtained from this algorithm closely matches the NSIDC SSM/I-derived 30% ice concentration extent.

Due to the different design, Seawinds measurements do not contain the information needed to obtain an estimate of σ^o incidence angle dependence. Also, since the vertical and horizontal σ^o data are at different incidence angles the polarization ratio is undefined for Seawinds. Regardless, the Seawinds σ^o measurements are sensitive to the presence of sea ice as shown in the next section.

SEAWINDS SEA ICE DETECTION

Since both NSCAT and Seawinds have similar Ku-band frequencies and spatial resolutions, Seawinds images can be simulated from NSCAT SIRF images. For this study Eq. (1) is used to simulate Seawinds enhanced resolution $A_v(55)$ and $A_h(47)$ images from NSCAT images,

$$A_v(55) = A_v - B_v(55° - 40°) \tag{4}$$

$$A_h(47) = A_h - B_h(47° - 40°). \tag{5}$$

Since Seawinds κ images can be created in an identical manner as NSCAT, the NSCAT κ images are used.

The Seawinds design precludes using γ or B_v. However, $A_v(55)$ and $A_h(47)$ contain useful information about the presence of sea ice. Although these two σ^o measurements are taken at different incidence angles, their ratio,

$$\gamma_{sw} = AV_{55} / AH_{47}, \tag{6}$$

is still somewhat sensitive to the presence of sea ice although less sensitive than γ for NSCAT. All combinations

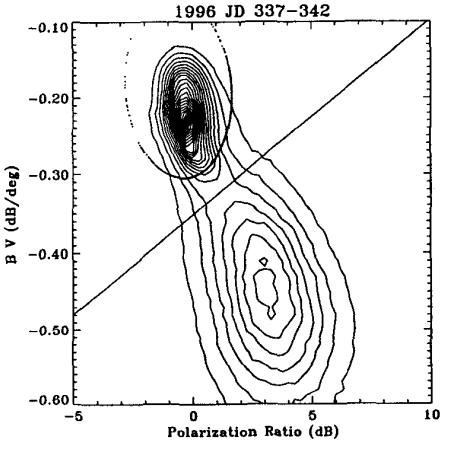

Figure 1: Contour plot of the distribution of NSCAT γ vs. B_v values for 1996 JD 337-342 with the associated decision boundaries. The upper left mode is sea ice, the other represents ocean pixels.

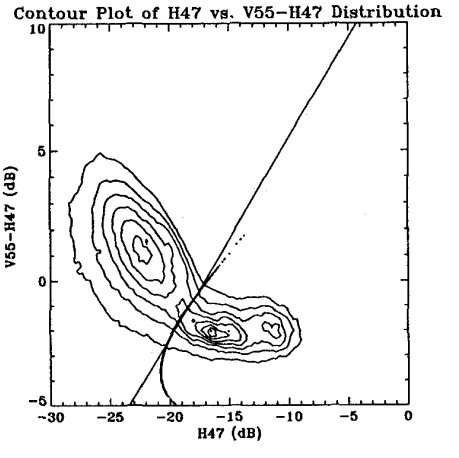

Figure 2: Contour plot of the distribution of Seawinds $A_h(47)$ vs. $A_v(55)/A_h(47)$ (in dB) along with its discriminant boundaries.

of $A_v(55)$, $A_h(47)$, and γ_{sw} as primary discrimination parameters are tested for discrimination ability. The best combination is γ_{sw} and $A_h(47)$ since the modes of the bimodal distributions are most distinct in this case. Figure 2 shows an example γ_{sw} vs. $A_h(47)$ distribution contour plot and discrimination boundaries. The distribution is clearly bimodal although there is more overlap between the ice and ocean modes than in the NSCAT distribution shown in Figure 1. Using these two parameters, the ice extent algorithm is applied once again using κ as a correction factor. Due to the increased modal overlap, more frequent classification errors are expected. The ice detection algorithm is applied using these primary classification parameters with similar κ correction.

The NSCAT algorithm is applied to Antarctic simulated Seawinds data. Four representative data periods from the NSCAT mission were chosen at different times of the Antarctic melt cycle to ensure algorithm stability through the dynamic seasonal ice cycle. The time frames are 1996 JD 307-312, 1996 JD 337-342, 1997 JD 4-9, and 1997 JD 34-39. The ice mapping algorithm was used to estimate the ice extent for all four test periods. Figure 3 shows the resulting edges plotted against each other for one of the time frames. The Seawinds edge provides a good estimate of ice edge; however, it is more susceptible to errors in some cases. Unfortunately, the information provided by the scatterometer in these instances does not provide the polarization response and incidence angle dependence that is so valuable in ice detection.

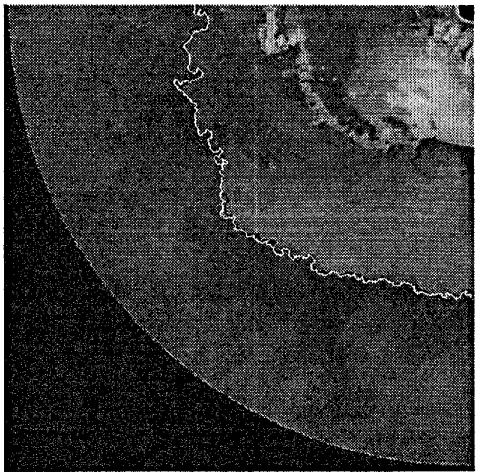

Figure 3: Edge comparison plots for the lower left quadrant of the Antarctic image with day range 1996 JD 337-342. The black and white edges correspond with the NSCAT and Seawinds estimates, respectively.

CONCLUSION

The sea ice detection algorithm designed for use with NSCAT data can be adapted for use with data collected from the Seawinds scatterometer. Although the instruments differ in design, the data can still be used to detect sea ice in the polar regions. The Seawinds design can detect the ice extent with a fair degree of accuracy. However, the lack of polarization response and σ^o incidence angle dependence in this data makes the Seawinds detection more likely to missclassify pixels. Still, Seawinds data will be useful in augmenting Special Sensor Microwave Imager data in the detection of sea ice.

An advantage of the Seawinds instrument over NSCAT is the increased coverage of the earth's surface. Seawinds has a wider swath than NSCAT and has no nadir gap allowing Seawinds polar images to be produced using only 1-2 days of data rather than the 6 days required for NSCAT. As a result, the ice extent maps can be produced on 1-2 day intervals with quality similar to the NSCAT 6 day ice extent estimates. In this case, sea ice dynamics become less of a factor in discrimination errors near the edge.

REFERENCES

[1] D. Long and M. Drinkwater, "Greenland Ice-Sheet Surface Properties Observed by the Seasat-A Scatterometer at Enhanced Resolution," *J. of Glaciology*, vol. 40, no. 135, pp. 213–230, 1994.

[2] S.H. Yueh, R. Kwok, S. Lou, and W. Tsai, "Sea Ice Identification Using Dual-Polarized Ku-Band Scatterometer Data," *IEEE Trans. on Geosci. and Rem. Sens.*, vol. 35, no. 3, pp. 560–569, May 1997.

[3] Q.P. Remund and D.G. Long, "Automated Antarctic Ice Edge Detection Using NSCAT Data," *Proc. of IGARSS '97*, Singapore, v. 4, pp. 1841-1843.

[4] F.M. Naderi, M.H. Freilich, and D.G. Long, "Spaceborne Radar Measurement of Wind Velocity Over the Ocean–An Overview of the NSCAT Scatterometer System," *Proc. of the IEEE*, vol. 79, no. 6, pp. 850–866, June 1991.

[5] Spencer, M.W., C. Wu, D.G. Long, "Tradeoffs in the Design of a Spaceborne Scanning Pencil Beam Scatterometer: Applications to SeaWinds," *IEEE Trans. on Geosci. and Rem. Sens.*, vol. 35, no. 1, pp. 115-126, 1997.

[6] D. Long, P. Hardin, and P. Whiting, "Resolution Enhancement of Spaceborne Scatterometer Data," *IEEE Trans. on Geosci. and Rem. Sens.*, vol. 31, pp. 700–715, 1993.

ACKNOWLEDGMENTS

NSCAT data provided by PO.DAAC at the Jet Propulsion Laboratory.